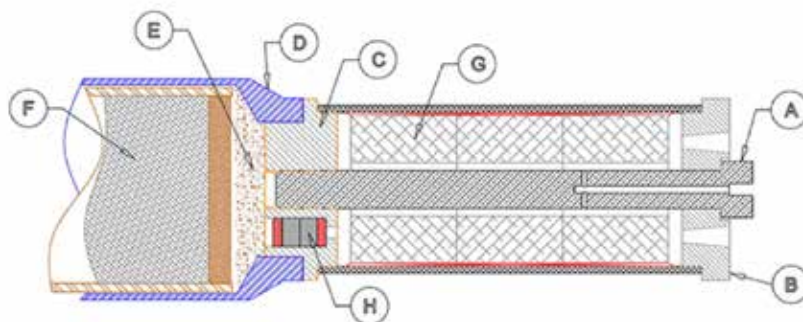


June 29, 2015

This signal delay is intentional.

Pyrotechnic delays prevent launched signal flares from igniting too close to the ground to be useful. Conventional pyrotechnic delays rely on perchlorates, chromates, barium, lead, and other environmentally problematic materials, that burn slowly enough without extinguishing in the large, flat delay housings typical of Army handheld signals.



Signal rocket schematic

The figure is a schematic of a signal rocket. The rocket motor (G) and delay element (C) are ignited simultaneously. The delay element burns for several seconds before it ignites the black powder expelling charge (E), which ignites and ejects the pyrotechnic payload (F). The article contains a full description of the signal rocket.

A. P. Shaw and co-workers at the US Army RDECOM-ARDEC* (Picatinny Arsenal, NJ) ran prototype tests of a more environmentally benign pyrotechnic delay based on boron carbide (B_4C), sodium periodate ($NaIO_4$), and polytetrafluoroethylene (PTFE) that burns at rates between 1 and 21 s/cm, depending on stoichiometry, particle size, and how tightly the columns are packed.

In dynamic tests on fully assembled signal rockets, the delay time was consistently 46% shorter than for static tests on stand-alone delay elements. The authors attribute this finding to the pressure and heat within the rocket combustion chamber as the propellant burns. Because the B_4C - $NaIO_4$ -PTFE mixture releases a substantial amount of gaseous combustion products, conductive and convective heat transfer propagate the burn front. Hot combustion gases carry away any condensed-phase products, leaving the housing almost empty and continuously exposing the column burn front. Thus, a slow-burning composition (14–15 wt% B_4C) is required to achieve the desired 5–6 s dynamic delay time.

The authors tested their system at -54 and $+71$ °C to confirm its reliability and safety at extreme ambient temperatures. Impact, friction, and electrostatic discharge tests confirmed that the B_4C -based delay is insensitive to unintended ignition. The ignition temperature is 475 °C, well above the decomposition temperature of $NaIO_4$ and the melting points of $NaIO_3$ and PTFE. (*ACS Sustainable Chem. Eng.* DOI: 10.1021/acssuschemeng.5b00254; Nancy McGuire)

*Research, Development and Engineering Command–Armament Research, Development and Engineering Center

June 22, 2015

Microbial balance affects sea spray composition.

Sea spray aerosol (SSA) particles affect the Earth's climate because they scatter solar radiation and seed cloud formation. These effects can change when ocean phytoplankton blooms release insoluble organic material that mixes with the sea salt particles in the aerosol. Scientists' understanding of the mechanisms that control the transfer of organic matter from seawater to SSA is limited, and currently it is not possible to predict the organic composition of SSA.

K. A. Prather at the University of California, San Diego, and the Scripps Institution of Oceanography (San Diego) and colleagues at these institutions and the University of Iowa (Iowa City), Colorado State University (Fort Collins), the National Institute of Oceanography and Experimental Geophysics (Trieste, Italy), Xiamen University (China), the University of Wisconsin—Madison, and the University of California, Davis, studied organic matter in SSA produced from a 3400-gal sample of natural seawater in a laboratory wave channel (shown in the figure).



Wave channel lab facility

The researchers added nutrients to the seawater that spurred two phytoplankton blooms over a 29-day period. They produced SSA by creating breaking waves in the wave channel. The first bloom enriched the aliphatic organic content (including lipids) of submicrometer SSA in proportion to the increasing abundance of phytoplankton, which they tracked by monitoring chlorophyll a concentrations. Ice nucleation in the SSA particles increased concurrently with this bloom.

A second phytoplankton bloom did not enrich organic species in the submicron SSA droplets. Heterotrophic bacteria concentrations, however, were much higher during the second bloom, possibly fed by the lipids from the first bloom. The authors believe that bacterial enzymes degraded the lipids to less active, more soluble species (likely fatty acid salts) that were transferred less efficiently into the submicrometer SSA droplets.

A kinetic model suggests that enhanced SSA organic content depends on a delicate balance between the rate at which phytoplankton produce labile lipids and the rate at which bacterial enzymes degrade these lipids. This helps explain the conflicting results from field studies that investigated the factors that control organic content in SSA and their effects on climate properties. (*ACS Cent. Sci.* DOI: 10.1021/acscentsci.5b00148; Nancy McGuire)

Copyright © 2015 American Chemical Society

June 15, 2015

Composite bone cement keeps its cool while setting. Common treatments for painful vertebral compression fractures (a problem associated with osteoporosis) currently require injecting a poly(methyl methacrylate) (PMMA) bone cement into the fractures. As the cement polymerizes and hardens, it releases large amounts of heat, which kills the surrounding tissues.

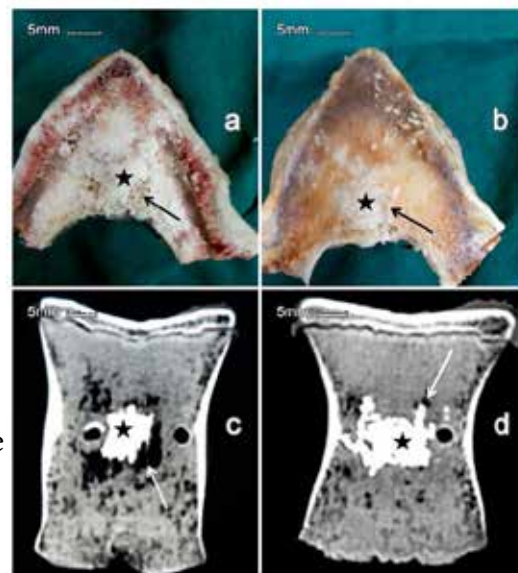
F. Zhou, D. Qiu, Z. Yang, and colleagues at Peking University Third Hospital (Beijing), the Chinese Academy of Sciences (Beijing), Soochow University (Suzhou, China), and the University of the Chinese Academy of Sciences (Beijing) mixed paraffin-containing silica microcapsules with PMMA cement powder to form a composite material. As the cement sets, the paraffin melts and absorbs much of the heat given off by the PMMA. Enclosing the paraffin in microcapsules prevents it from leaking into the surrounding cement and tissues.

The microcapsules are compatible with the surrounding cement matrix; no gaps were observed between the microcapsules and the matrix after polymerization. The microcapsules retain their spherical shape, which demonstrates their toughness and resistance to leakage.

The composites take longer to set than plain PMMA cement, but only when the composite contains >20 wt% microcapsules (PMMA20) does the setting time become excessive for use with surgical procedures. The composite cements have significantly lower compressive strength and compressive modulus than PMMA alone. This property could be advantageous because it allows better matching of these properties between the cement and the surrounding bone material and reduces the probability of stress fractures in the bone.

Biocompatibility is similar for the PMMA20 and plain PMMA, but the composite material produces a much smaller thermal necrosis zone. In the figure, a and b are optical images of the bovine lumbar vertebrae implanted with PMMA and PMMA20, respectively. Images c and d are the corresponding coronal CT images of the necrosis zone 24 h after injection of the cement samples. The arrows point to the thermal necrosis zone and stars (★) mark the positions of implanted cements. The PMMA20-treated bone has far fewer pores than the PMMA-treated one.

The authors believe that composite cement that contains 20 wt% paraffin may be suitable for use in percutaneous vertebroplasty and balloon kyphoplasty procedures. They recommend that the cement be further evaluated. (*ACS Appl. Mater. Interfaces* DOI: 10.1021/acsami.5b01447; Nancy McGuire)

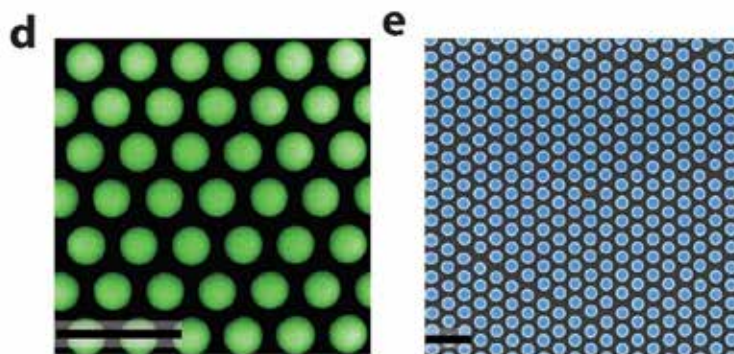


a and c: PMMA-treated beef bone, with tissue damage. b and d: PMMA20-treated bone, with less tissue damage.

June 8, 2015

Monolayer mask makes metamaterial mirrors. Metamaterials, conventional metals or plastics that are engineered to form crystal-like periodic structures, have unique physical properties, including the ability to channel light waves. Ideally, these properties arise from their structural features rather than the material from which they are made.

The disadvantages of the optical-frequency performance of metal-based metamaterials are free-carrier absorption and anisotropic optical response. Scaling up the production of metal metamaterials is not economical because of the slow, expensive nanolithography processes required to pattern them. Dielectric metamaterials provide lower losses and simpler structural geometries, making them an attractive alternative.



Etch mask (left) and metamaterial array (right)

J. Valentine and coauthors at Vanderbilt University (Nashville, TN), SRI International (Menlo Park, CA), and Oak Ridge National Laboratory (TN) produced centimeter-size samples of an all-dielectric metamaterial based on cylindrical silicon resonators. Their metamaterial is a “perfect” reflector (99.7% at 1530 nm), and it operates in the telecommunications frequency (S or short-wave) band.

The authors used a monolayer hexagonal close-packed lattice of polystyrene spheres as an etch mask (left in the figure) on a silicon-on-insulator substrate. Chemically etching the silicon and removing the mask produced a hexagonal array of silicon cylinders. (right)

Unlike metal mirrors, the metamaterial reflector acts as a magnetic mirror in which magnetic field lines cause moving particles to reverse direction. This occurs when the magnetic mode is spectrally separated from the electric mode. This separation can be achieved by keeping the periodicity and height of the cylinders the same and reducing the diameter of the cylinders to increase their physical separation.

Some disorder occurs during the preparation of these dielectric metamaterials, but it does not adversely affect their performance. The materials can be designed for narrowband or broadband performance. The assembly method is simple, inexpensive, and rapid. (*ACS Photonics* DOI: 10.1021/acsphotonics.5b00148; Nancy McGuire)

Copyright © 2015 American Chemical Society

June 1, 2015

How does fluoride in groundwater affect forage plants? Fluoride ion occurs naturally in groundwater and soil, but agricultural and industrial activities can elevate these levels considerably. Livestock that drink water and eat forage plants with high fluoride concentrations are at risk of developing fluorosis, a condition with symptoms ranging from a harmless discoloration of the teeth to brittle, malformed bones.

P. M. Kopittke and coauthors at the University of Queensland (St. Lucia) and Santos (Brisbane, both in Australia) conducted a laboratory and field study of soil fluoride levels and forage plant uptake in Australia's Great Artesian Basin. They examined fluoride adsorption in soils, its release into the groundwater, plant root uptake and transport to leaf tissues, and accumulation of fluoride in the leaf tissues.

The seven soils in the study varied substantially in their capacity to adsorb fluoride. Enough fluoride reentered the groundwater to kill the plants growing in washed white quartz sand, the weakly-adsorbing control soil. Red ultisol (red clay soil) released an intermediate amount of fluorine; yellow ultisol and red vertisol (expansive clay) released the least. In red ultisol and sand, fluorine was present predominantly as free fluoride ion, but it occurred as Al-F complexes in the yellow ultisol.

Fluoride accumulation in plant leaf tissues was greatest for the sand and least for red vertisol. Leaf concentrations of fluoride did not depend on the total concentration of fluoride in the soil solution for Rhodes grass (*Chloris gayana*) or leucaena (*Leucaena leucocephala*), but there was a weak correlation for Lucerne (*Medicago sativa*).

The authors found no consistent relationship between fluoride speciation, soil solution concentration, and accumulation in leaf tissues across all of the examined soil types and plant species. Lucerne leaves, however, retained a significant amount of fluoride from overhead irrigation with fluoride-containing water. The other plant species retained more modest amounts. Lucerne tissues also showed the greatest loss of fluoride after being rinsed with deionized water.

Even in soils that contained the equivalent of irrigation with 0.26 mM fluoride solution at 5 ML/(ha·year) for 25 years, most plant tissues contained fluoride levels below the maximum tolerable level for mature beef cattle, sheep, chickens, and swine. For an 8-year-equivalent concentration, plant fluoride levels were still acceptable for young beef calves and heifers. The authors note that further studies are needed to evaluate other soils, plant species, and fluoride concentrations. (*J. Agric. Food Chem.* DOI: 10.1021/acs.jafc.5b01001; Nancy McGuire)

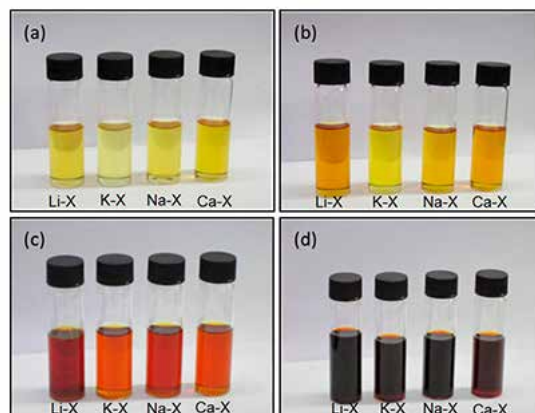
Copyright © 2015 American Chemical Society

May 25, 2015

Zeolite nanocrystals inhibit palm oil oxidation. Palm oil represents 30% of global vegetable oil output, but it has low thermal and oxidative stability, and it is prone to hydrolysis. Oxidation products from heated cooking oils such as palm oil may pose a health risk.

Nanosized zeolite crystals prepared without a templating agent are nontoxic and suitable for use as food additives. They are used to filter out impurities and oxidation products from oils so that they can be reused. This study shows that zeolites can also retard oxidation.

S. Mintova at the University of Caen (France), E.-P. Ng at the University of Science, Malaysia (Penang), and coauthors in Malaysia, France, Indonesia, Singapore, and Bulgaria studied palm oil to which 0.5 wt% zeolite M-X (M= Li⁺, Na⁺, K⁺, or Ca²⁺) was added. They stirred the mixtures at 150 °C and drew samples at 100, 200, 300, and 400 h to follow the oxidative evolution of each oil sample with several analytical techniques.



Zeolite additive keeps palm oil fresh.

A reference oil that contained no zeolite changed color from yellow to black and developed a strong smell over the course of the experiment. The discoloration rates of the zeolite-containing oil samples were inversely correlated with the polarizability of the zeolite counterion: fastest to slowest, Li⁺ > Na⁺ > Ca²⁺ > K⁺. NMR spectroscopy showed that zeolites with highly basic cations were better at slowing the formation of aldehydes and carbonyl compounds. The figure shows the color changes for each oil sample from (a) 100 h to (d) 400 h. Color change for each oil–zeolite sample over time

Oxidation products with polar acidic groups attract other organic molecules to form bulkier molecules, which increase the oil's viscosity. Zeolite counterions with low charge densities (K⁺ and Na⁺) were better at protecting the oils from viscosity changes by slowing the formation of polymeric oxidized compounds.

Zeolites that contained Ca²⁺ and K⁺ were best at hindering the formation of hydroxyl compounds, and all of the zeolites slowed the generation of water during oxidation. Ca²⁺ was best at stabilizing hydroperoxides, the primary oxidation product, which slowed the formation of secondary oxidation products (alcohols, aldehydes, ketones, carboxylic acids, and esters). Divalent Ca²⁺ also was most effective in adsorbing oxidation products from the oils; and it formed salts with the carboxylic acids to reduced oil acidity.

Periodic density functional theory calculations showed that the zeolite counterions interacted preferentially with hydroperoxide oxidation products rather than the C=C bonds in the oil molecules. The calculations predicted that Ca²⁺ would be most effective at hindering oxidation, but the experiments placed it behind K⁺. (*J. Agric. Food Chem.* DOI: 10.1021/acs.jafc.5b00380; Nancy McGuire)

May 18, 2015

New method makes better structure—property predictions. Process design requires an understanding of the thermodynamic properties of the materials involved. When data on these properties are unavailable, a quantitative structure–property relationship (QSPR) regression method can establish relationships between molecular properties and the thermodynamic properties of interest. These relationships can be updated and refined as new data become available.

W. H. Carande and colleagues at the National Institute of Standards and Technology (Boulder, CO) and the University of Colorado Boulder used support vector regression (SVR) to estimate critical properties and acentric factors (a measure of nonsphericity) for 900 pure compounds. They used experimental data on three-dimensional geometry and connectivity to calculate >500 molecular descriptors for each compound. These were used to define the input vectors for the SVR calculations.

Optimal SVR parameters produced results that were as close as possible to target values based on experimental data for critical temperatures, critical temperature/critical pressure ratios, and reduced saturation pressures (related to the acentric factor). The authors showed that the effective use of the available information in large experimental datasets requires many variables: 11 to 33 in the current study. Descriptors based on charge distributions were especially influential in the calculations, as were some descriptors related to vibrational and spectroscopic analysis.

The methods used in this study calculated critical property values that were closer to the observed values than those generated in a previous study by the same research team. The authors attribute the improvement to expansions and corrections to the molecular descriptor dataset and better model generation.

The dataset for the current study used only experimental values. This eliminated the overfitting problem observed in other recent studies that used predicted and observed data. (*J. Chem. Eng. Data* DOI: 10.1021/je501093v; Nancy McGuire)

Copyright © 2015 American Chemical Society

May 11, 2015

How hazardous are lead-containing solar cells? Methylammonium lead(IV) iodide ($\text{MeNH}_3\text{PbI}_3$) films form the basis of affordable, high-voltage hybrid organic–inorganic perovskite (HOIP) solar cells. When $\text{MeNH}_3\text{PbI}_3$ is exposed to water, it decomposes to form lead(II) iodide (PbI_2), which is several orders of magnitude more water-soluble than other commonly used solar panel materials. The lead-containing films in solar cells could be encapsulated to limit contact with the environment, but damaged solar cells could release lead.



Do lead-containing solar panels present a pollution hazard?

G. Hodes, D. Cahen, and co-workers at the Weizmann Institute of Science (Rehovot, Israel) exposed $12\text{ mm} \times 30\text{ mm}$ $\text{MeNH}_3\text{PbI}_3$ films to water at pH values from 4.2 to 8.1 to mimic the effects of rain on exposed films in solar panels. They determined the degree of lead loss with gravimetric measurements and inductively coupled plasma mass spectrometry analysis.

Exposing the films to water vapor caused hydrate formation, which could be reversed by heating the samples. After only a few seconds of contact with liquid water, however, the samples decomposed completely and irreversibly.

The authors calculated that a 1-m^2 panel having a 300-nm thick $\text{MeNH}_3\text{PbI}_3$ layer contains $\approx 0.4\text{ g}$ of lead. Releasing all the lead from a field of solar panels would add $\approx 70\text{ ppm}$ of lead to the first centimeter of soil beneath the panels. (Lead levels in soil typically range from $<10\text{ ppm}$ in pristine areas to 200 ppm or more in urban areas.)

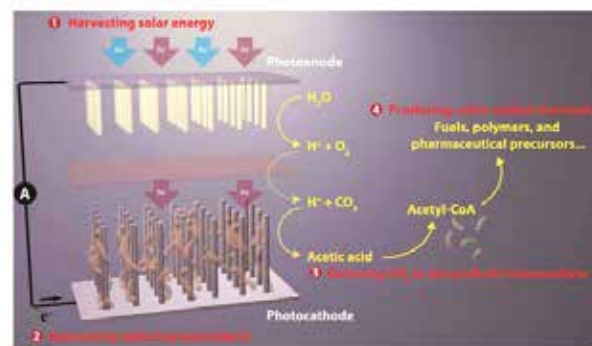
The authors compared the potential for lead contamination with the lead output from coal-fired electric power plants. They concluded that if breakage does not exceed one solar module in 300 over a period of 20 years, the amount of lead released would be less than from the least polluting coal-fired plants over the same time frame. They also noted that the lead from coal-fired plants is released into the atmosphere, whereas the lead from HOIP solar panels can be collected and recycled. (*J. Phys. Chem. Lett.* DOI: 10.1021/acs.jpcllett.5b00504; Nancy McGuire)

Copyright © 2015 American Chemical Society

May 4, 2015

A nanowire–bacteria hybrid achieves artificial photosynthesis.

For millions of years, plants have used solar power to produce value-added biochemicals from carbon dioxide and water. The inability of the enzymes that catalyze CO₂ reduction to self-repair outside of a cellular environment has hindered attempts to replicate this process artificially. These enzymes often do not tolerate oxygen, which limits their use with CO₂ sources such as flue gas. Selecting biosynthetic intermediates to use as building blocks also has been difficult.



Bacteria colony in a nanowire array performs photosynthesis

M. C. Y. Chang, P. Yang, and colleagues at the University of California, Berkeley; Lawrence Berkeley National Laboratory; and Kavli Energy NanoSciences Institute (Berkeley) developed a biocompatible nanowire array that captures sunlight and provides a direct interface with microbial colonies. They used this system to produce acetic acid, which they then converted to precursors of fuels, polymers, and pharmaceutical compounds.

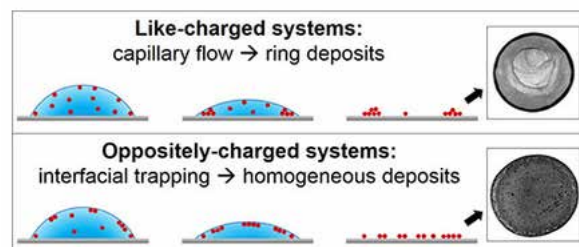
A photoanode array made of titanium dioxide nanowires collects ultraviolet light and releases electrons to a silicon nanowire photocathode array. A colony of the anaerobic bacterium *Sporomusa ovata* forms an interconnected network in the local anaerobic environment created by the photocathode array. Buffered brackish water containing trace amounts of vitamins is used as a culture medium. An ion-conductive membrane between the anode and cathode separates the reaction products. Platinum is used as an electrocatalyst to reduce oxygen in the feed gas.

The *S. ovata* colony reduces CO₂ and water to acetic acid at ambient temperature at a rate comparable with that of conventional gas-phase catalysts operating at temperatures >100 °C. With an inorganic electrolyte, the acetic acid titer is ≈20 mM within 5 days; and it can reach >100 mM in an M9-MOPS medium (Teknova, Hollister, CA). Some efficiency is lost when the source gas contains oxygen, but this can be mitigated by improving the design of the nanowire–bacteria hybrid.

As a proof of concept, specific strains of genetically engineered *Escherichia coli* (housed in a separate reactor) were used to convert the acetic acid to acetyl coenzyme A. This enzyme served as a building block to form 1-butanol, poly(hydroxybutyrate) polymer, and three natural isoprenoid compounds (amorphadiene, epiaristolochene, and cadinene). (*Nano Lett.* DOI: 10.1021/acs.nanolett.5b01254; Nancy McGuire)

April 27, 2015

Charge balance gets rid of “coffee rings”. The coffee-ring effect bedevils inkjet printing, cDNA microarrays, and other technologies that rely on solvent evaporation to deposit particles uniformly onto a substrate. Suspended particles migrate to the edge of a droplet as it evaporates, producing ring-shaped deposits. Strategies used to control particle flow patterns and produce more uniform deposits include controlling particle shapes and adding cosolvents, polymers, or surfactants.



Charge balance prevents particle migration to evaporation front, deposits particles evenly

M. Anyfantakis, D. Baigl, and colleagues at Paris Sciences and Letters Research University, Pierre and Marie Curie University, and the National Center for Scientific Research (all in Paris) observed the evaporation behavior of microliter-size droplets that contained suspended solid particles and surfactants. They showed that surfactant-mediated electrostatic interactions between particles and the liquid interfaces, rather than flow patterns, determined how the particles were deposited.

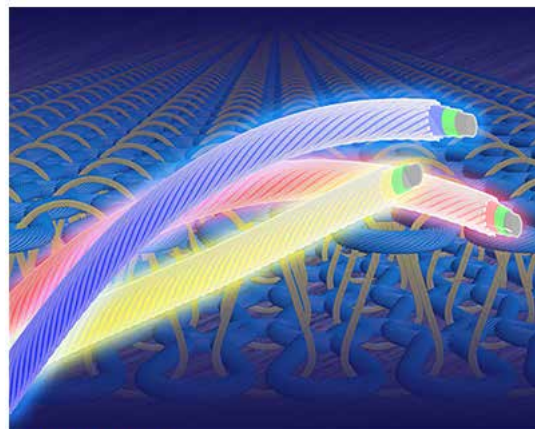
When the solid particles and the surfactant have like electrical charges, the surfactant has very little influence on the particle deposition pattern. Radial evaporation-driven capillary flow dominates, and particles migrate to the edge of the droplet. When the suspended particles and the substrate (or a layer of surfactant adsorbed onto the substrate) have opposite charges, a few particles adhere to the substrate near the center of the droplet, but most of the particles are deposited in rings.

When particles and surfactant have opposite charges, however, the surfactant adsorbs onto the particle surfaces. Coffee rings persist at high and low concentrations of surfactant where the coated particles have the net electrical charge of the surfactant or of the particle, respectively. At intermediate concentrations, the surfactant charge balances the charge on the particles, making them more hydrophobic. These coated particles form a dense skin on the surface of the droplet that is not affected by radial capillary flow for most of the evaporation process. Thus, the particles are deposited as a uniform disk (see figure).

The authors observed this behavior in a variety of mixtures, regardless of the absolute charge and surface chemistry of the particles or the charge and hydrophobicity of the surfactants. (*Langmuir* DOI: 10.1021/acs.langmuir.5b00453; Nancy McGuire)

April 20, 2015

Modern-day knights might wear shining cardigans. Modern-day knights might wear shining cardigans. Light-emitting fibers that can be woven or knitted into fabrics may potentially be used for many things, from safety clothing for night-time walkers and cyclists to medical devices. H. Peng and coauthors at Fudan University (Shanghai), Shanghai University, and the University of California, Los Angeles, developed fibers that function as polymer light-emitting electrochemical cells (PLECs). These fibers efficiently produce light and require very little power.



Courtesy of H. Peng

Light-emitting fibers can be woven or knitted into fabrics

The researchers dip-coated a thin stainless steel wire, the cathode, with a layer of zinc oxide (ZnO) nanoparticles. A second dip-coating deposited an electroluminescent polymer layer. They then wrapped an outer layer of aligned carbon nanotubes, which served as a transparent anode, around the outside of the polymer coating.

The ZnO layer reduces current leakage and prevents the metal from fluorescence-quenching the polymer layer. The polymer layer contains the blue-light-emitting polyfluorene copolymer PF-B, the ethoxylated trimethylolpropane triacrylate electrolyte ETT-15, and the salt lithium trifluoromethanesulfonate.

The resulting ≈ 1 mm-thick fibers can be twisted or woven into textiles. When a potential of a few volts is applied between the metal wire and the carbon nanotube layer, the entire fiber surface emits light. Coating fibers with polymers that emit different colors and connecting them to independently variable external current sources allowed the resulting colors to be tuned continuously and independently over a wide range (see figure).

Previous attempts at making LECs were limited by the contact arrangement of the electrodes or the small scale of the fibers. This study overcomes these limitations, although the fibers require ≈ 21 min to achieve maximum luminescence. The intensity decreases slowly over the next 4 h. Repeated bending of the fibers does not decrease their performance, which the authors demonstrated by weaving light-emitting fabrics.

Future development work will concentrate on increasing operating stability. Other improvements could include generating other colors, scaling up production, and developing an outer protective coating material for the fibers. (*Nat. Photonics* DOI: 10.1038/nphoton.2015.37; Nancy McGuire)

Copyright © 2015 American Chemical Society

April 13, 2015

Chameleons use photonic crystals to change color. Chameleons use photonic crystals to change color. Most species that change color rapidly do so by dispersing or aggregating pigment-containing organelles to modify skin brightness. Only a few species, including chameleons, actually change their skin hue. This usually requires cellular structures that modify light wave reflectance and interference, rather than pigment cells.



A calm chameleon

J. Teyssier, S. V. Saenko, and co-workers at the University of Geneva (Switzerland) used electron microscopy, photometric videography, and photonic band-gap modeling to show that panther chameleons from Madagascar change color by tuning a lattice of guanine nanocrystals. The researchers examined biopsied skin samples 2 mm in diameter. They used Raman spectroscopy to identify two types of dark chromatophores that contain melanin and an unidentified dark blue pigment that panther chameleons of both sexes and all ages use to modulate skin color in response to stress (see video, <https://www.youtube.com/watch?v=XdQvtP8EKrM>).

Adult males can produce more extreme color shifts when they encounter a male competitor or a receptive female. They have a thick upper skin layer with iridophores (reflective or iridescent cells) that contain close-packed lattices of small guanine crystals. The crystal arrays and surrounding cytoplasm behave as photonic crystals, similar to those that generate bright colors in some birds and insects. Transmission electron microscope images of skin samples show that the distance between guanine crystals is 30% smaller in the resting state (blue to green) than in the excited state (yellow to white).

A deeper skin layer contains iridophores with larger guanine crystals that reflect a substantial portion of sunlight, especially in the near-infrared range, which may protect the chameleons from overexposure to the sun in their native hot, dry habitats. (*Nat. Commun.* DOI: 10.1038/ncomms7368; Nancy McGuire)

Copyright © 2015 American Chemical Society

April 13, 2015

This 3-D process makes parts at a rapid CLIP. Additive manufacturing, or 3-D printing, has captured the imagination of parts manufacturers and do-it-yourselfers alike. The process, however, is very slow; it requires the sequential deposition of hundreds of thin layers. A new process, continuous liquid interface production (CLIP), produces monolithic polymeric shapes with dimensions of tens of centimeters and resolved features $<100\ \mu\text{m}$ across in minutes rather than hours.



E. T. Samulski, J. M. DeSimone, and coauthors at Carbon 3D (Redwood City, CA), the University of North Carolina (Chapel Hill), and North Carolina State University (Raleigh) formed complex solid shapes by projecting a continuous sequence of ultraviolet (UV) images through an oxygen-permeable window located below a liquid polymer resin bath. The oxygen inhibits free-radical polymerization by creating a “dead zone”, or continuous liquid interface, several tens of micrometers thick on the lower surface of the resin.

New 3D fabrication method pulls complex shapes from liquid polymer

As the part is continuously drawn out of the resin bath, the UV-exposed regions (which contain residual free radicals) move out of the oxygen-rich zone, polymerize, and harden; and a new liquid layer forms underneath. The sequence of the UV images determines the shape of the part's cross-section at each level. The speed of the process, which can reach 500 mm/h, is limited by the polymer's cure rate and viscosity rather than by stepwise layer formation.

The authors experimented with various dead-zone thicknesses, polymerization rates, and feature resolutions to establish optimum conditions and limitations of the technique. An amorphous fluoropolymer, Teflon AF 2400, makes a good oxygen-permeable window. Pure oxygen forms a thicker dead zone than air; pure nitrogen produces no dead zone at all.

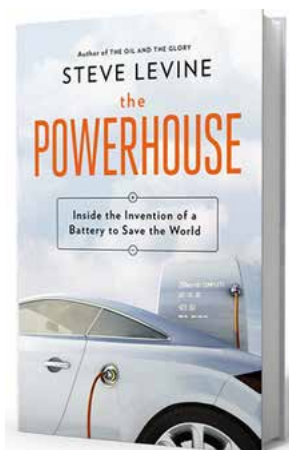
Increasing the incident photon flux or the reactivity of the polymer resin reduces the thickness of the dead zone. Dye loading can increase feature resolution by inhibiting print-through effects. Because the dyes absorb UV light that would otherwise produce free radicals, however, the parts must be elevated more slowly to increase light exposure and solidify the polymer adequately.

Other recently published preliminary studies show that the CLIP process can be used to produce parts from soft elastic materials, ceramics, and biomaterials. (*Science* DOI: 10.1126/science.aaa2397; Nancy McGuire)

Copyright © 2015 American Chemical Society

April 6, 2015

The race for high-performance lithium batteries continues. Science isn't done in a vacuum. The scramble for funding, egos and personalities, grad students and postdocs who come and go—all of these factor into what gets done, how well, and how quickly. Steve LeVine, the Washington, DC, correspondent for Quartz and a Future Tense fellow at the New America Foundation (Washington, DC), wrote a recently released book based on 2 years of “unprecedented access” to Argonne National Laboratory’s lithium battery research team. He tells of the team’s bid to lead the Battery Hub, a national research effort focused on developing high-performing lithium batteries for vehicles and, eventually, for power storage for homes and businesses.



The Powerhouse, by Steve Levine

The Argonne team sought to model their research methods after Bell Laboratories. They recruited the nation’s best minds and worked to understand the science at the most basic levels. The effort to land the Hub contract brought Argonne scientists together with a startup company called Envia Systems (Newark, CA) and Argonne’s erstwhile rivals at the University of California, Berkeley.

LeVine gained extensive access to the scientists at Argonne and Envia, who gave him a candid account of the difficult journey from basic research to market-ready product and of the competition between the United States, Japan, Korea, and China to dominate this market. LeVine also touches on the geopolitical implications of a crash in petroleum demand should electric cars come to dominate the market.

He includes just enough crystallography and electrochemistry to give nonscientists a general idea of the technology and scientists a starting point for seeking more detailed information. His account of discoveries and setbacks should be familiar to anyone who has encountered the “technology transfer valley of death”.

LeVine also portrays the outsize egos, long work hours, and the “large role of [BS]” involved in the making of a major invention. He paints a sympathetic portrait of scientists and engineers led astray by their own beliefs and the administrators and businessmen who fudged the facts to get funding and customers. (LeVine, S. *The Powerhouse: Inside the Invention of a Battery to Save the World*; Viking Penguin: New York, 2015; Nancy McGuire)

Copyright © 2015 American Chemical Society